Deformation and Collapse of Microtubules on the Nanometer Scale

P. J. de Pablo, I. A. T. Schaap, F. C. MacKintosh, and C. F. Schmidt

Division of Physics and Astronomy, Vrije Universiteit, De Boelelaan 1081, 1081 HV Amsterdam, The Netherlands

(Received 21 April 2003; published 27 August 2003)

We probe the local mechanical properties of microtubules at the nanometer scale by radial indentation with a scanning force microscope tip. We find a linear elastic regime that can be described by both thin-shell theory and finite element methods, in which microtubules are modeled as hollow tubes. We also find a nonlinear regime and catastrophic collapse of the microtubules under large loads. The main physics of protein shells at the nanometer scale shows simultaneously aspects of continuum elasticity in their linear response, as well as molecular graininess in their nonlinear behavior.

DOI: 10.1103/PhysRevLett.91.098101 PACS numbers: 87.16.Ka, 87.15.La, 87.64.Dz

Microtubules (MT) are among the principal components of the cytoskeleton, the dynamic structural framework of cells [1]. MTs are cylindrical shells of about 25 nm diameter, formed by a regular helical lattice of α-β tubulin dimers, noncovalently joined by protein-protein bonds. Alternatively one can view MTs as constructed of 13 parallel protofilaments joined laterally. Their length can vary from tens of nanometers to hundreds of microns.

The mechanical properties of MTs play a crucial role in processes such as intracellular transport and cell division. MT elastic properties have been studied previously by observing the thermal fluctuations of MT shape [2], by actively bending the MT with optical tweezers [3], and by observing bending against membranes or hard surfaces [4]. Bending experiments typically probe length scales much greater than the size of the protein subunits. At this micrometer (i.e., cellular) scale, the bending of MTs is well described by the continuum mechanics of elastic rods [5,6], although there remains considerable uncertainty over the value of the bending rigidity. MTs have also been modeled as elastic shells before to study GHz acoustic excitations [7].

Here, we probe the mechanics of single MTs locally by radial indentation with a scanning force microscope (SFM) tip, directly observing their local, tubelike structure. SFM has been used recently to measure MTs mechanical properties [8]. These experiments, however, probed only bending modes of MTs. Using the Hertz model (valid only for solid bodies), Vinckier *et al.* [9] found an apparent Young's modulus (extrapolated to zero glutaraldehyde concentration) of about 3 MPa, which is substantially smaller than what we find by taking into account the tubelike structure of MTs. Thus, in prior MT experiments it has not been possible to probe their hollow structure. Furthermore, it was previously found that MTs were too fragile to withstand the interaction with the tip and they had to be strongly cross-linked with glutaraldehyde. Here we were able to image and manipulate microtubules without chemical cross-linking.

Tubulin was purified from porcine brain following established recipes [10]. MTs were polymerized, diluted in the presence of taxol [11] to avoid their depolymerization [12], and attached to glass coated with aminopropyltriethoxy-silane as described before [13]. To image MTs in buffer, the SFM (Nanotec^{TM}) was operated in jumping mode [14]. We used cantilevers with a spring constant of 0.05 N/m and a tip radius of about 20 nm (OMCL-RC-800PSA, Olympus. Japan). The minimal loading force (50 pN) is given by the thermal noise of the cantilever [15].

Figure 1(a) shows a typical MT imaged with SFM at a maximal force of 50 pN. The measured height of around 25 nm matches with the 25 nm diameter observed in electron microscopy studies [16]. In order to investigate the mechanical properties of MTs, the tip was positioned

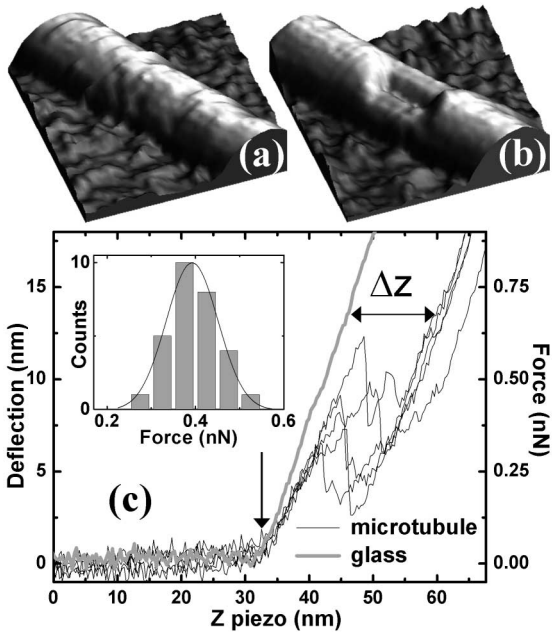

FIG. 1. (a) shows a typical SFM image of an MT before performing a set of FZs. In (b) a hole can be observed at the spot of the microtubule where the FZs where performed. (c) shows a typical set of FZ performed on an MT. The inset shows a histogram of the force where the nonlinear regime begins. A peak is found at 400 pN.

on top of a single MT as judged from a directly preceding image, and several force versus distance curves (FZ) [black curves in Fig. 1(c)] were performed at the same spot at a constant sampling rate and constant velocity. At a maximum force of ~1 nN the number of FZs, which can be performed at one spot until the MT is destroyed [Fig. 1(b)] was up to ~5. Once the contact between the MT and the tip is established [see arrow Fig. 1(c)], the FZ curve is linear up to a certain critical force. At a force that varies between repeated attempts and between different microtubules over a range from ~300 to ~500 pN [inset of Fig. 1(c)], the FZ curves showed catastrophic discontinuities. In control experiments we found no evidence of measurable adhesion forces between tip and microtubules (data not shown).

We will first focus on the quantitative interpretation of the linear elastic regime. The cantilever deflection [vertical axis in Fig. 1(c)] is related to the force exerted by the tip via the known cantilever stiffness of 0.05 N/m. The signal reporting the cantilever deflection is calibrated by performing an FZ on glass [gray curve in Fig. 1(c)]. The indentation depth Δz [Fig. 1(c)] is calculated from the z difference between the MT and the glass curves at a given force. A number of averaged indentation curves in the linear regime from five MTs and a linear regression are shown in Fig. 2(a), demonstrating a linear elastic regime up to an indentation of ~4 nm. The effective spring constant is $k = 0.100 \pm 0.005$ N/m. Indentation of a semi-infinite solid object is commonly described by the Hertz model [17], which due to geometry, has no linear response. The geometry in our case is different, and the Hertz model is not applicable because the MT is a hollow cylindrical shell that can bend, buckle, and collapse, which a solid object cannot do. In the present case a linear dependence of the force on the indentation depth is expected for deformations of the order of the shell thickness [5,18].

The linear elastic deformation of curved shells in general involves coupling of out-of-plane bending with in-plane compression [5,18]. An exceptional case is that of a hollow cylinder that can flatten under a extended radial load, by bending without compression. For a uniform cylindrical shell of thickness t this deformation is governed by a bending modulus given by $\kappa = Et^3/[12(1-\nu^2)]$, where ν is the Poisson ratio and E is the Young's modulus [5]. Apart from a geometric prefactor of order unity, (d/R^2) measures the deviation of the local curvature away from the equilibrium cylindrical shape (radius R), where d is the indentation depth. The bending energy therefore scales as $Et^3(d/R^2)^2R$ per unit length of the tube.

As the cylinder becomes longer the total bending energy, assuming homogeneous flattening, grows without limit. Under a point load, the cylinder will therefore return to its undistorted shape at a certain distance from the point of loading. For long, thin-walled cylinders (i.e., to leading order in t/R) the zone of deformation extends a distance $\ell > R$ along the axis from the point of force application, as can be quantitatively determined from the analytic solution [Fig. 2(b)]. In a scaling approach, we can illustrate the essential physics and estimate the relevant length scales by minimizing the total elastic energy associated with the deformation. Given a nonuniform indentation along the cylinder axis, there is a longitudinal, in-plane displacement u along the axis of the cylinder that is proportional to the indentation d, but also must decrease with increasing ℓ/R. In fact, analytic results [19] show that $u \approx Rd/\ell$, and hence the strain is of order Rd/ℓ^2. This results in an approximate, combined elastic energy

$$U_{\text{tot}} = Et^3(d/R^2)^2R\ell + Et(Rd/\ell^2)^2R\ell. \qquad (1)$$

Minimization of U_{tot} leads to $\ell \approx R\sqrt{R/t}$. Thus, the dominant or softest mode of deformation of the cylinder surface extends along the axis far away from the point of force application. The local flattening of the cylinder extends thus roughly $R\sqrt{R/t}$ along the axis and R in the other direction. We expect from this result that our experiments will not be very sensitive to the SFM tip radius, so long as it is comparable to the MT radius.

Since U_{tot} is harmonic in the indentation d, we obtain an effective spring constant given by $Et^{5/2}/R^{3/2}$, apart from a prefactor of order unity. From the complete analytic solution obtained within the classical theory of shells [18,19], we calculate that the spring constant k_S

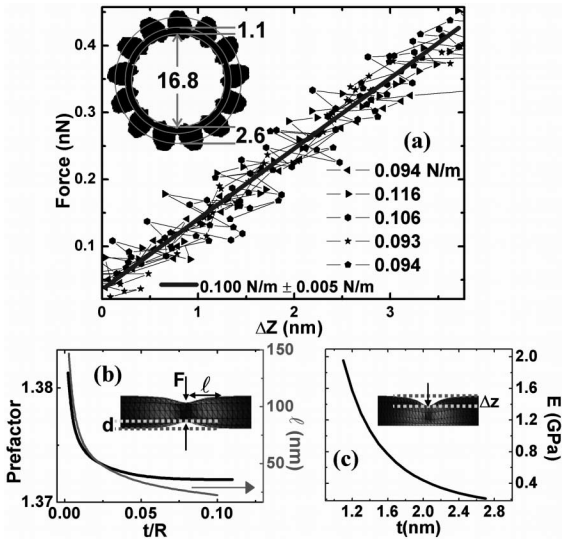

FIG. 2. (a) shows the indentation of five MTs in the linear regime, with their calculated spring constants. Inset of (a) shows the cross section of an MT based on electron microscopy data 21. In (b) the prefactor for $k \propto Et^{5/2}/R^{3/2}$ is plotted vs t/R. The gray line represents the effective deformed length ℓ. Both of them are plotted from the analytical solution for a symmetrically deformed tube, as sketched. (c) shows the Young's modulus versus the effective wall thickness t using Eq. (3).

for the case of equal and opposite point forces f is about

$$k_S = f/d \cong 1.37Et^{5/2}/R^{3/2} \quad (2)$$

to within 1% over the range $0.002 < t/R < 0.1$ [Fig. 2(b)]. This does not exactly correspond to the experimental situation where the tip applies a force f from one side while the MT is supported by a flat surface from the other side, and where the observed change in height Δz [inset of Fig. 2(c)] is an apparent change in diameter of the cylinder. The deformations and forces are computed for finite-length cylindrical sections in the correct experimental geometry using finite element methods (CADRE, cadrepro4.2^{TM}). The model based on a 3D tube consists of 12 609 plates, each of which is treated within a thin-shell approximation with a Poisson ratio of 0.3. For small displacements we confirm the scaling behavior of Eq. (2) up to about $t/R \approx 0.1$ (appropriate for MTs), but with a somewhat different prefactor,

$$k_S = f/\Delta z \cong 1.18Et^{5/2}/R^{3/2}. \quad (3)$$

This corresponds to a stiffer spring, taking into account the fact that the height change Δz should be compared with $2d$. It is interesting to consider the corresponding expression for spherical surfaces [5], where $k_S \approx Et^2/R$. The effective spring constant for the indentation of cylinders is weaker by a factor of $\sqrt{t/R} < 1$, because of the ability of the cylinder to flatten without much in-plane compression. The additional rigidity of spherical surfaces is related to a classical theorem due to Jellett [20] that says that closed spherical (or more generally, ellipsoidal) surfaces are completely rigid if they are inextensible.

We now explore the implications of the model for our experimental data. We expect that the indentation response reveals a different aspect of microtubule mechanics from prior bending experiments. Microtubules are rather structured and far from being homogeneous shells. The structure of MTs is known to atomic resolution from electron microscopy [inset of Fig. 2(a)]. One evident feature is the existence of deep grooves between the protofilaments, while the inside surface as well as the top of an individual protofilament is rather flat [21]. Given this complex structure, it is clear that indenting experiments are testing very different properties than bending experiments. Flexural rigidity is determined by the full thickness of the protofilament and the overall tube diameter, while indentation is primarily sensitive to the thin bridges between the protofilaments where the strain will be concentrated. In order to compare our results to bending experiments we estimate an effective Young's modulus of the microtubule wall from our data. To apply our model, we have to assume an effective wall thickness somewhere between the radially averaged wall thickness and the thickness of the bridges between the protofilaments [inset of Fig. 2(a)]. In Fig. 2(c) the Young's modulus, calculated from the experimental spring constant k using expression (3), is plotted versus the assumed effective wall thickness running from 1.1 to 2.6 nm and was found to be $\sim$1 Gpa.

In order to refine our result, we carried out a finite element calculation for a cylindrical tube reinforced with longitudinal beams, mimicking the protofilaments [19], and introducing anisotropy in a homogeneous tube. Using the experimental $k = 0.1$ N/m, the calculation results in a Young's modulus of about $\sim$0.8 GPa. This value corresponds to an effective wall thickness of $\sim$1.6 nm [close to the 1.1 nm bridge thickness shown in Fig. 2(a)] in the homogenous tube model [Fig. 2(c)]. This confirms that the bridges dominate the elastic response. Even though we examine a different mode of deformation and do so at the nanometer scale, the Young's modulus we derive, given the known geometry of the MT, is consistent with the results from prior bending experiments [6].

In the following we discuss the nonlinear regime of the measured elastic response [Fig. 1(c)]. The sudden decrease of force is likely caused by either one of two processes: slipping off of the tip from the MT onto the glass substrate or MT collapse. The force necessary to make the tip slip is difficult to estimate since it would depend on the exact position of the tip over the MT and on the attachment of the MT to the substrate. The vertical distance moved should in that case, however, account for the full diameter of the MT. For a collapsed MT, in contrast, some material would be present between the tip and the glass. The inset of Fig. 3 shows a typical indentation curve. Given the variation in these individual indentation curves, we also show an indentation histogram of 23 such curves on five different MTs (all at the same approach velocity and sampling rate). This histogram demonstrates a clear pattern of stages in the indentation. The peak (i) represents the linear regime of indentation. Since the distance

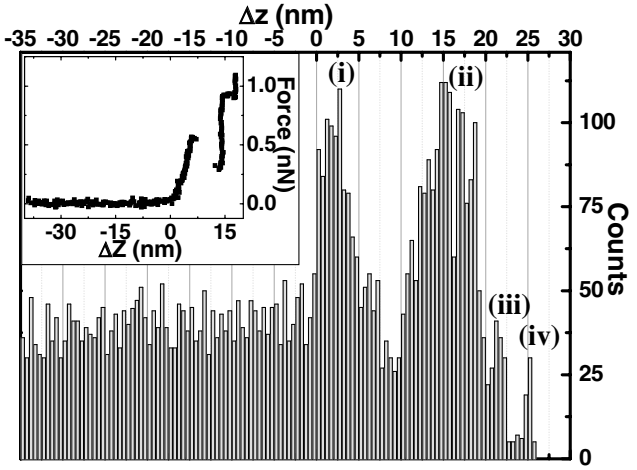

FIG. 3. The indentation curve of a single FZ is plotted in the inset, showing two jumps. The MT is indented for positive values of the x axis. The histogram of 23 indentation curves performed on five MTs is showing four different peaks, corresponding to the different deformation states of the MT.

moved between the point of first contact and the peak (ii) is ~15 nm, which is about the inner diameter of a 13 protofilaments MT [Fig. 2(a)], the peak (ii) most likely reflects a collapsed double layer of tubulin between the tip and the glass. We also expect to see two other possible indentations: (1) corresponding to a single layer of tubulin, and (2) to bare glass. There is evidence for these in the peaks on the right of the histogram [(iii) and (iv)]. No indentations beyond 25 nm from contact were observed. In the histogram is evident that the full indentation of 25 nm was rarely seen, indicating that slip off or complete breakthrough were rare.

In conclusion, we have used the nanometer sized SFM tip to indent microtubules, and found a linear elastic response with an apparent spring constant $k = 0.1$ N/m up to a deformation of about 4 nm, comparable to the shell thickness [22]. The elastic response is well described by models of the MTs as isotropic cylindrical shells made from a homogeneous material. Taking into account the deeply grooved structure of MTs, we estimate a Young's modulus of 0.8 GPa. Characteristically for cylindrical shells and in contrast with spherical shells, these microtubules are expected to flatten under a point load over a large length of order $R\sqrt{R/t}$, which is large compared with the cylinder radius of order 10 nm. Indentation probes locally the protein structure of MTs in a very different way from bending experiments. Radial indentation is very sensitive to the circumferential corrugations of the shell, and therefore complements bending experiments that mainly depend on axial structure formed by the protofilaments. While we have here focused on the physical properties of MTs, we are also strongly interested in the biological functional implications of these material properties. The forces needed to deform locally MTs are only about an order of magnitude larger than the force a single motor protein can exert, and are thus in the range of biologically relevant forces. Interestingly, the radial stiffness of MTs will also be a sensitive function of the binding of microtubule associated proteins, particularly the ones that bind in the grooves between the protofilaments [23].

We acknowledge fruitful discussions with D. Schaap, J. van Mameren, E. Peterman, G. Sgalari, and T. Smith, and financial support from the Dutch Foundation for Fundamental Research of Matter (FOM) and ALW/FOM Project No. 01FB28/2.

[1] M. Schliwa, *The Cytoskeleton: An Introductory Survey* (Springer-Verlag, New York, 1986); S. Inoue and E. D. Salmon, Mol. Biol. Cell **6**, 1619 (1995); D. Boal, *Mechanics of the Cell* (Cambridge University Press, Cambridge, 2002); B. Alberts, A. Johnson, J. Lewis, M. Raff, K. Roberts, and P. Walter, *Molecular Biology of the Cell* (Garland Science, New York, 2002).

[2] F. Gittes, B. Mickey, J. Nettleton, and J. Howard, J. Cell. Biol. **120**, 923 (1993).

[3] H. Felgner, R. Frank, and M. Schliwa, J. Cell Sci. **109**, 509 (1996).

[4] M. Elbaum, D. K. Fygenson, and A. Libchaber, Phys. Rev. Lett. **76**, 4078 (1996); M. Dogterom and B. Yurke, Science **278**, 856 (1997).

[5] L. D. Landau and E. M. Lifshitz, *Theory of Elasticity* (Pergamon Press, New York, 1986).

[6] J. Howard, *Mechanics of Motor Proteins and the Cytoskeleton* (Sinauer, Sunderland, 2001).

[7] Y. M. Sirenko, M. A. Stroscio, and K.W. Kim, Phys. Rev. E **53**, 1003 (1996).

[8] A. Kis, S. Kasas, B. Babic, A. J. Kulik, W. Benoit, G. A. D. Briggs, C. Schonenberger, S. Catsicas, and L. Forro, Phys. Rev. Lett. **89**, 248101 (2002).

[9] A. Vinckier, C. Dumortier, Y. Engelborghs, and L. Hellemans, J. Vac. Sci. Technol. B **14**, 1427 (1996).

[10] R. C. Williams, Jr. and J. C. Lee, Methods Enzymol. **85**, 376 (1982).

[11] The role of taxol in the mechanical properties of MT remains unclear, with prior experiments showing both increased and decreased rigidity. B. Mickey and J. Howard, J. Cell Biol. **130**, 909 (1995); see also Ref. [3].

[12] I. Arnal and R. H. Wade, Curr. Biol. **5**, 900 (1995).

[13] P. J. de Pablo, I. A. T. Schaap, and C. F. Schmidt, Nanotechnology **14**, 143 (2003).

[14] F. Moreno-Herrero, P. J. de Pablo, R. Fernandez-Sanchez, J. Colchero, J. Gomez-Herrero, and A. M. Baro, Appl. Phys. Lett. **81**, 2620 (2002).

[15] F. Gittes and C. F. Schmidt, Eur. Biophys. J. **27**, 75 (1998).

[16] D. Chretien and R. H. Wade, Biol. Cell **71**, 161 (1991).

[17] K. L. Johnson, *Contact Mechanics* (Cambridge University Press, Cambridge, 2001).

[18] F. Niordson, *Shell Theory* (North-Holland, New York, 1985).

[19] I. A. T. Schaap, P. J. de Pablo, F. C. MacKintosh, and C. F. Schmidt (to be published).

[20] J. H. Jellett, Roy. Irish Acad. Trans. **22**, 343 (1855).

[21] H. Li, D. J. DeRosier, W. V. Nicholson, E. Nogales, and K. H. Downing, Structure **10**, 1317 (2002); K. H. Downing (private communication).

[22] A linear response has also been shown to be possible for the indentation of bacteria, due primarily to turgor pressure [M. Arnoldi, M. Fritz, E. Bauerlein, M. Radmacher, E. Sackmann, and A. Boulbitch, Phys. Rev. E **62**, 1034 (2000)].

[23] H. Felgner, R. Frank, J. Biernat, E. M. Mandelkow, E. Mandelkow, B. Ludin, A. Matus, and M. Schliwa, J. Cell Biol. **138**, 1067 (1997).